EFFECT OF NEAR-WALL TURBULENCE ON MIXING HYDRODYNAMICS

V. M. Barabash, L. N. Braginskii,
R. Z. Liv'yant, and V. L. Sadovskii

UDC 66.063:532.54

The distribution of the circumferential liquid velocity in units with mixing devices was investigated theoretically in the presence of fixed internal devices of arbitrary geometry. The tangential stresses on the casing of the unit were evaluated by using Landau's model of attenuation of turbulence near solid surfaces, and the turbulent exchange of the momentum moment was described on the basis of Prandtl's "mixing path" theory. A calculation method is proposed which is applicable for units with mixing devices of different types in a wide range of change of geometric correlations and designs. The analytical results were confirmed by comparison with the experimental data.

The existing concepts of the mechanism of momentum transfer in turbulent streams and the semiempirical models based on them make it possible to analyze in simplified form the mechanism of formation of some characteristics of a velocity field [1], in particular, the profile of the circumferential velocity in units with mixing devices. The distribution of the circumferential velocity component of the medium being mixed in a steady regime should satisfy the principle of conservation of momentum.

Let us isolate in the unit a unit volume of liquid in the form of an annular element of radius r, thickness dr, and height h. The equation of equilibrium of the moments applied to the considered element can be represented in the following form:

$$dM_{to}-dM_t-dM_r=0, \quad \text{or} \quad dM_t=dM_{to}-dM_r, \tag{1}$$

where dM_{to} is the torsion moment applied to a unit volume as a result of its interaction with the mixer blades, J; dM_t is the difference of the moments created by tangential stresses on cylindrical surfaces of radii r and (r + dr), J; and dM_r is the moment of hydraulic-resistance forces which appears during interaction of the circumferential stream with segments of the bottom and internal devices included between surfaces r and (r + dr), J.

Since the value of dM_{to} is variable with respect to the radius of the unit, in the general case we assume

$$dM_{to}=\varphi(r)\,dr, \tag{2}$$

where $\varphi(r)$ is the function of the distribution density of the torsion moment with respect to the radius, J/m.

In the zone affected by the liquid agitated by the mixer blades, the moment dM_{to} can be expressed by the difference of the liquid and mixer velocities, and in the remaining part of the unit $dM_{to} = 0$. Thus, during mixing with a mixing device having the number of blades z_b

$$\varphi(r)=\begin{cases} z_b\xi_b\dfrac{\rho(\omega_0 r-v(r))^2}{2}h_b r & \text{for} \quad r\in\Omega_m, \\ 0 & \text{for} \quad r\notin\Omega_m, \end{cases} \tag{3}$$

where Ω_m is the set of values of the radii on which direct interaction of the stream with the mixer blades occurs.

Let us express the increase of the moment of friction forces between neighboring liquid layers by the tangential stress τ:

$$dM_t=2\pi Hd(r^2\tau(r)), \tag{4}$$

Leningrad Scientific-Research and Construction Institute of Chemical Equipment. Translated from Teoreticheskie Osnovy Khimicheskoi Tekhnologii, Vol. 20, No. 6, pp. 798-804, November-December, 1986. Original article submitted October 22, 1984.

0040-5795/86/2006-0501$12.50

where $\tau(r)$ is the tangential stress on a surface with radius r, Pa. To determine τ, meaning an approximate analysis, let us use the hypothesis of Prandtl's mixing-path length, which, for the case of a twisted stream with small curvature of the stream lines, leads [2] to the expression

$$\tau=\rho l^2\frac{\partial v}{\partial r}\left|\frac{\partial v}{\partial r}\right|. \tag{5}$$

Taking into account that in units with mixing devices without reflecting baffles the change of the circumferential liquid velocity with respect to height is insignificant [3], we replace the partial derivatives in (5) by ordinary ones. The mixing path length l can be assumed (by analogy with [4, 5]) to be equal to the width of the turbulent-mixing zone:

$$l=\alpha L,\quad L=\begin{cases} r_m & \text{for} \quad 0\leqslant r\leqslant r_m,\\ R-r_m & \text{for} \quad r_m\leqslant r\leqslant R,\end{cases} \tag{6}$$

where r_m is the radius corresponding to the maximum on the curve of the radial profile of the circumferential liquid velocity, m, and α is the proportional coefficient.

With due regard for (4)-(6), we have

$$dM_t=2\pi H\rho\alpha^2L^2d\left[r^2\frac{dv}{dr}\left|\frac{dv}{dr}\right|\right]. \tag{7}$$

In the general case, the term dM_r in (1) is the sum

$$dM_r=dM_{in}+dM_{bo}. \tag{8}$$

The resistance moment applied to a unit volume of liquid as a result of its interaction with fixed internal devices is

$$dM_{in}=\psi(r)\,dr, \tag{9}$$

where $\psi(r)$ is the function of the distribution density of the resistance moment of internal devices:

$$\psi(r)=\begin{cases}\sum\limits_{i\ in}\zeta_i\rho\dfrac{v^2(r)}{2}h_ir & \text{for} \quad r\in\Omega_{in},\\ 0 & \text{for} \quad r\notin\Omega_{in}\end{cases} \tag{10}$$

Here Ω_{in} is the set of values of the radii on which direct interaction of the circumferential stream with internal devices occurs.

In the case of a flat bottom

$$dM_{bo}=2\pi r^2\tau_{bo}(r)\,dr. \tag{11}$$

Thus, with due regard for (2), (7), and (11), the equation of equilibrium of the unit volume of liquid (1) assumes the form

$$2\pi H\rho\alpha^2L^2d\left[r^2\frac{dv}{dr}\left|\frac{dv}{dr}\right|\right]=\varphi(r)\,dr-\psi(r)\,dr-2\pi r^2\tau_{bo}(r)\,dr$$

or

$$\frac{d}{dr}\left[r^2\frac{dv}{dr}\left|\frac{dv}{dr}\right|\right]=\frac{\varphi(r)-\psi(r)-2\pi r^2\tau_{bo}(r)}{2\pi H\rho\alpha^2L^2}. \tag{12}$$

As uniqueness conditions in the integration of Eq. (12), let us use the correlation

$$v(r)=\omega_0r_s \quad \text{for} \quad r=r_s \tag{13}$$

and the integration condition for the equilibrium of the moments

$$M_{to}=M_{in}+M_{bo}+M_{wa}, \tag{14}$$

where

$$M_{to}=\int_0^R\varphi(r)\,dr; \tag{15}$$

$$M_{in}=\int_0^R \psi(r)\,dr; \tag{16}$$

$$M_{bo}=2\pi\int_0^R r^2\tau_{bo}(r)\,dr; \tag{17}$$

r_s is the radius of the mixer shift, m. The resistance moment of the cylindrical wall of the unit's casing is

$$M_{wa}=2\pi RH\tau_{wa}. \tag{18}$$

To solve Eqs. (12)-(18), we need the values of the tangential stress on the walls and bottom of the unit. In [3, 6], Braginskii and Begachev propose the equation

$$\tau_{wa}=\rho c_f v_{wa}^2/2, \tag{19}$$

where c_f is the resistance coefficient determined [6] with the empirical relation

$$c_f=\lambda_t \mathrm{Re}^{-0.25}. \tag{20}$$

where λ_t is a coefficient, and Re = $v_{av}R/\nu$ is the Reynolds number.

However, also possible is a theoretical evaluation of c_f based on the use of Landau's hypothesis [7] about the nature of attenuation of turbulence near solid surface and also the Kolmogorov–Obukhov theory of locally isotropic turbulence [8, 9].

The momentum transfer in a turbulent boundary layer near a solid surface is usually described by the equation

$$\tau=\rho(\nu+\nu_t)(dv/dy), \tag{21}$$

where ν_t is the turbulent viscosity, m^2/sec, and y is the distance from the wall, m.

Let us express the tangential stress as

$$\tau=v/R_\tau, \tag{22}$$

where v is the liquid velocity far from the wall, m/sec, and R_τ is the resistance to momentum transfer

$$R_\tau\simeq\int_0^\infty dy/\rho(\nu+\nu_t). \tag{23}$$

Assuming that the main resistance to momentum transfer is concentrated in the viscous sublayer [2, 10], for determination of ν_t we use Landau's hypothesis [7], assuming the change of the turbulent viscosity in the viscus sublayer to be proportional to the fourth degree of the distance from the wall:

$$\nu_t=\nu(y/\delta_0)^4. \tag{24}$$

With due regard for (24), the integration of expresssion (23) leads to the relation

$$R_\tau=\left(\frac{\pi}{2\sqrt{2}}\right)\left(\frac{\delta_0}{\rho\nu}\right). \tag{25}$$

The thickness of the viscous sublayer δ_0 is related to the value of the characteristic pulsational velocity v_0 by the familiar correlation [10]

$$v_0\delta_0/\nu=11.5. \tag{26}$$

Hence, in accordance with (22) and (25),

$$\tau/v=0.078\rho v_0. \tag{27}$$

Usually the main difficulty in the calculation of processes of transfer to the wall consists in establishment of the relation of v_0 to the characteristics of macroscale flow. To solve this problem, let us assume that the intensity of turbulent transfer in the viscous sublayer, just as in the stream core [1, 11], is determined mainly by velocity pulsations of maximum scale. In the considered case, this scale should be of the order of thickness of the viscous sublayer δ_0, i.e., it is significantly less than the stream scale. At the same time, in accordance with (26), this scale exceeds the internal turbulence scale λ_0 corresponding to the condition

$$v_{\lambda_0}\lambda_0/\nu \simeq 1. \tag{28}$$

where $v\lambda_0$ is the pulsation velocity of scale λ_0, m/sec.

Thus, in order of magnitude, δ_0 corresponds to the region of scales for which the two-thirds law is applicable [8, 9]:

$$v_0^2 \simeq \varepsilon_{0\ell}^{2/3}\delta_0^{2/3}, \tag{29}$$

where $\varepsilon_{0\ell}$ is the local value of the energy dissipation in a unit of mass, W/kg, which, in a first approximation, can be replaced by the average value

$$\varepsilon_0 = N/(\rho V_\ell) = K_N n^3 d_m^5/V_\ell, \tag{30}$$

where V_ℓ is the volume of the medium in the unit, m^3.

Comparing (22), (25), (26), and (29), we obtain for τ and dM_{bo}:

$$\tau_{bo}(r) = 0.144\rho(\varepsilon_0\nu)^{0.25}v(r); \tag{31}$$

$$dM_{bo} = 0.288\pi\rho(\varepsilon_0\nu)^{0.25}v(r)r^2dr. \tag{32}$$

When (32) is used, the equilibrium equation of the unit volume of the liquid (12) acquires the form

$$\frac{d}{dr}\left[r^2\frac{dv}{dr}\left|\frac{dv}{dr}\right|\right] = \frac{\varphi(r) - \psi(r) - 0.288\pi\rho(\varepsilon_0\nu)^{0.25}v(r)r^2}{2\pi H\rho\alpha^2L^2}. \tag{33}$$

Correlations (13)-(18) are used as the uniqueness conditions for integration of (33).

Let us rewrite (17) with due regard for (31):

$$M_{bo} = 0.288\rho\pi(\varepsilon_0\nu)^{0.25}\int_0^R v(r)r^2\,dr. \tag{34}$$

The resistance moment of the cylindrical wall of the unit's casing M_{wa} is determined according to (18). In this case, by analogy with (31), the value of $\tau = \tau(R)$ is determined as

$$\tau(R) = 0.144\rho(\varepsilon_0\nu)^{0.25}v(R), \tag{35}$$

where v(R) is the circumferential liquid velocity at radius $r = R - \delta_0$, m/sec.

Since in units without internal devices the resistance moment of the cylindrical wall of the casing significantly exceeds the resistance moment of the bottom, and the values of $c_f = f(Re)$ measured in [6] reflect mainly the resistance characteristics of the wall, we use (35) for theoretical evaluation of the hydraulic resistance of the unit's wall. From a comparison of (19) and (35), it follows that the resistance coefficient of the casing is

$$c_f = 0.288(\varepsilon_0\nu)^{0.25}v(R)/v_{av}^2, \tag{36}$$

or

$$c_f = 0.288\varepsilon_0^{0.25}v(R)R^{0.25}\,\mathrm{Re}^{-0.25}/v_{av}^{1.75}. \tag{37}$$

With respect to the nature of the effect of the Reynolds number, this equation is analogous to relation (20), and in addition

$$\lambda_t = 0.288\varepsilon_0^{0.25}v(R)R^{0.25}/v_{av}^{1.75}. \tag{38}$$

The values of λ_t calculated according to this equation on the basis of the results of an experimental measurement of the circumferential velocities and power for $\bar{R} \geq 1.5$ are close to the averaged value of 0.095 (Fig. 1) found in [12] directly by means of the resistance and the average liquid velocity. These results indicate the possibility of theoretical determination of the tangential stress τ.

Thus, Eqs. (33), (13), and (14) are a closed system containing only one unknown parameter requiring experimental determination, the constant α in the expression for the mixing path length (6). For numerical solution of this system of equations, let us introduce the notation

$$z = r^2\frac{dv}{dr}\left|\frac{dv}{dr}\right|, \tag{39}$$

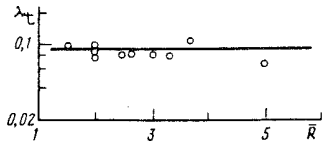

Fig. 1

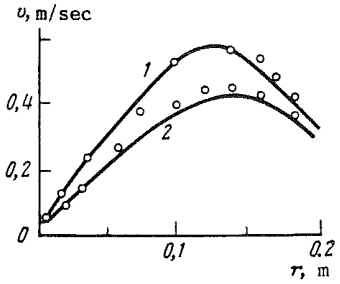

Fig. 2

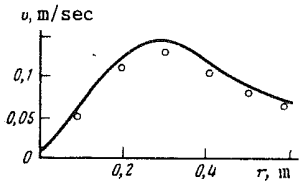

Fig. 3

Fig. 1. Relation of the coefficient λ_t to $\bar{R}$ at $\bar{R} \geq 1.5$. The points denote the calculation according to (38).

Fig. 2. Velocity profile in a 0.4-m-diameter unit. Gate mixing device, r_0 = 0.15 m; b_b = 0.021 m; H = 0.4 m. The medium is an aqueous glycerol solution (ν = 0.000017 m^2/sec): 1) ω_0 = 6.35 rad/sec; 2) 4.4. The solid lines denote the calculation; the points denote the experiment.

Fig. 3. Velocity profile in a 1.2-m-diameter unit with internal devices $\left(\sum_{z_{in}} \zeta_i f_i = 0.3RH\right)$. Blade mixing device, r_0 = 0.25 m, ω_0 = 1.15 rad/sec. The solid line denotes the calculation, and the points denote the experiment.

then

$$\frac{dv}{dr} = \frac{\sqrt{|z|}}{r} \operatorname{sign} z. \tag{40}$$

Taking into account (40) instead of (33), we can consider the system of first-order equations equivalent to it

$$\frac{dz}{dr} = \frac{\varphi(r) - \psi(r) - 0.288\pi\rho(\varepsilon_0\nu)^{0.25} v(r) r^2}{2\pi H \rho \alpha^2 L^2}, \quad \frac{dv}{dr} = \frac{\sqrt{|z|}}{r} \operatorname{sign} z \tag{41}$$

with boundary conditions (13) and (14).

This boundary problem was solved by the "shooting" method [13], which consists in reducing the solution of the boundary problem (41), (13), and (14) to a solution of the Cauchy problem. Assuming $z_0 = z(r_s)$ we obtain

$$\begin{gathered} \frac{dz}{dr} = \frac{\varphi(r) - \psi(r) - 0.288\pi\rho(\varepsilon_0\nu)^{0.25} v(r) r^2}{2\pi H \rho \alpha^2 L^2}; \\ \frac{dv}{dr} = \frac{\sqrt{|z|}}{r} \operatorname{sign} z; \\ v(r_s) = \omega_s r_s; \\ z(r_s) = z_0; \quad r_s \leq r \leq R. \end{gathered} \tag{42}$$

The solution of the Cauchy problem (42) amounts to finding a value of z_0 such that the condition of equality of the moments (14) would be satisfied. The value of z_0 is sought as follows. A physically justified interval, (a, b) = (10^{-18}, 1), containing z_0 is chosen. The function $\Delta = M_{to} - (M_{in} + M_{wa} + M_{bo})$. We assume z_0 to be equal successively to a and b. We solve the Cauchy problem (42) for each value of z_0, and we calculate Δ according to the obtained solution. At the ends of the interval (a, b), the function Δ assumes values of different signs. Further, over the first iteration we choose as z_0 the expression (a + b)/2 and for the chosen z_0 we solve problem (42), calculate Δ, and seek the new interval (a, b) and z_0 by the half-division method [13]. The calculations are continued until a value of z_0 is found for which $\Delta \leq \varepsilon$, where ε is a small number characterizing the accuracy of the solution. This means that boundary conditions (13) and (14) are satisfied and the initial problem (41) is solved.

The Cauchy problem is solved by the grid method [13]. Over the segment $[r_s, R]$ we use the uniform grid $\omega = \{r_i = ih, i = 0, 1, \ldots, N, h = (R - r_s)/N\}$. Then problem (42) is written

in difference form as

$$\frac{z_{i+1}-z_i}{h}=\frac{\varphi(r_i)-\psi(r_i)-0{,}288\pi\rho(\varepsilon_0\nu)^{0.25}v(r_i)r_i^2}{2\pi H\rho\alpha^2L^2};$$

$$\frac{v_{i+1}-v_i}{h}=\frac{\sqrt{|z_i|}}{r_i}\operatorname{sign}(z_i),\quad i=0,1,\ldots,(N-1);\tag{43}$$

$$v(0)=\omega_0 r_s;$$

$$z(0)=z_0.$$

The obtained system of algebraic equations is solved easily because the values of v_{i+1} and z_{i+1} at point r_{i+1} are defined completely by the values of v_i and z_i assigned at point r_i. Assuming successively i = 0, 1,..., (N − 1) we find the values of v_i and z_i for all $i \le N$.

We should note that in the solution of boundary problem (41) the value of α in (6) was assumed to be fixed and was determined as a result of comparison of the calculated and experimental relations v(r). The best correspondence between the calculated and experimental relations v(r) was obtained for α = 0.1. The results of comparison of the calculated curves with the experimental data (Figs. 2 and 3) indicate that the considered model describes the experimental results sufficiently well and can be used in the practice of engineering calculations.

NOTATION

b_b is the width of the blades of the gate and anchor mixing devices, m; d_m is the mixer diameter, m; f_i is the area of projection of the i-th internal device onto the vertical plane, m^2; H is the height of filling of the unit, m; h_i is the height of the i-th internal device, m; h_b is the height of the mixer blade, m; K_N is the power coefficient; N is the power consumed for mixing, W; n is the rotation rate of the mixing device, sec^{-1}; R is the radius of the unit, m; $\bar{R} = R/r_0$; r is the current radius, m; r_0 is the radius of the mixing device, m; v is the circumferential liquid velocity, m/sec; z_b is the number of mixer blades; z_{in} is the number of internal devices; ν is the kinetic viscosity, m^2/sec; ζ_b is the resistance coefficient of the mixer blade; ζ_i is the resistance coefficient of the i-th internal device; ρ is the density of the medium, kg/m^3; τ_{bo} is the tangential stress on the bottom of the unit, Pa; ω_0 is the angular velocity of the mixing device, rad/sec.

LITERATURE CITED

1. G. N. Abramovich, S. Yu. Krasheninnikov, A. N. Sekundov, and I. P. Smirnova, Turbulent Mixing of Gas Jets [in Russian], Nauka, Moscow (1974). p. 272.
2. Pai Shih-I, Turbulent Flow of Liquids and Gases [Russian translation], IL, Moscow (1962).
3. L. N. Braginskii, "Distribution of circumferential liquid velocities and depth of the whirlpool in units with mixing devices," Teor. Osn. Khim. Tekhnol., 1, No. 5, 583 (1967).
4. L. N. Braginskii, V. I. Begachev, et al., "Calculation of the homogenization time in smooth-walled units with mixing devices on the basis of a diffusion model," ibid., 8, No. 4, 590 (1974).
5. V. L. Sadovskii, L. N. Braginskii, and V. M. Barabash, "Use of semiempirical turbulence theories in calculation of velocity fields in units with mechanical mixing devices," in: Apparatus with Mixing Devices [in Russian], No. 80, NIIKhimmash, Moscow (1978), p. 13.
6. L. N. Braginskii and V. I. Begachev, "Interrelation between the circumferential liquid velocity and the power in mixing," Teor. Osn. Khim. Tekhnol., 6, No. 2, 260 (1972).
7. L. D. Landau and E. M. Lifshits, Continuum Mechanics [in Russian], Gostekhteorizdat, Moscow (1953).
8. A. N. Kolmogorov, "Energy dissipation in local isotropic turbulence," Dokl. Akad. Nauk SSSR, 32, No. 1, 19 (1941).
9. A. M. Obukhov, Izv. Akad. Nauk SSSR, Ser. Georg., 5, Nos. 4-5, 453 (1941).
10. L. G. Loitsyanskii, Mechanics of Liquids and Gases [in Russian], Nauka, Moscow (1973).
11. V. A. Kulukhov, V. M. Barabash, et al., "Investigation of the field of circumferential velocities and radial turbulent transfer in mixing under conditions characteristic of large units," Teor. Osn. Khim. Tekhnol., 9, No. 1, 48 (1975).
12. L. N. Braginskii, V. I. Begachev, V. P. Glukhov, and L. N. Volchkova, "Effect of viscosity on the circumferential liquid velocity in units with mixing devices," ibid., 5, No. 3, 446 (1971).
13. G. Korn and T. Korn, Handbook of Mathematics [Russian translation], Nauka, Moscow (1974).

POROUS ROTARY LIQUID SPRAYERS

A. A. Kolesnik and N. A. Nikolaev

UDC 621.43:66.069.83

A new type of porous rotary sprayers for spraying in narrow fractions was studied, and the principles of spraying liquids from the surface of porous rotary sprayers were formulated.

Spraying of liquids is widely used in the various branches of chemical technology for granulating melts, dehydrating solutions, and in many other processes. However, the jet and disk sprayers used at present for this purpose form polydispersed sprays which greatly complicate the processes and diminish the product quality. Therefore, the development of essentially new liquid sprayers for spraying in narrow fractions is a very real problem, the solution to which would enable appreciable intensification of such processes.

Several investigators studied the possibility of producing drops of uniform size by spraying liquids. The more successful among them was Schmidt [1] who, based on Hege's principle [2], was the first to use a porous rotary sprayer (PRS) made of cermets and obtain narrow fractions of sprays of many liquids. Gösselle [3] experimentally studied the output and operational regimes of PRS made of cermets and also determined the drop sizes formed on the sprayer surface with an average grain size of $0.7 \cdot 10^{-3}$ m.

The qualitative picture of spraying liquids using the PRS was studied in [1, 3] and many specifications for them were formulated:

the sprayer material should possess high porosity and mechanical strength;

when the porous material is wetted by the liquid sprayed, drop formation should occur on the grains and, when not wetted, on the outer pores;

the most suitable grain form is a sphere; the average grain diameter of the spraying body should be six times that of the given drop size when spraying a hydrophobic liquid; and

when spraying a hydrophilic liquid, the pore size should be double that of the desired drop size.

Though the results of [1, 3] represent the first important step toward designing an essentially new type of liquid sprayers, they do not adequately explain the drop formation mechanism and the selection of optimum grain form, PRS structure, and their most effective operational regimes. A thorough study was therefore made of the PRS operational principles.

A study of the properties of various porous materials helps conclude that synthetic porous materials produced from particles of proximate grain size, by pressure molding followed by baking into a finished article are most suitable for use in the chemical technology. Among these are the well-known solid filtering and abrasive materials like porous permeable ceramics, porous glass, and many polymers and abrasives.

Abrasive materials possessing the following properties are most suitable for a host of chemical engineering uses [4, 5]: high mechanical strength, inertness to a very wide range of corrosive liquids, and high thermal stability (up to 2000°C); fairly uniform grain size of abrasive material ($\delta^{max}/\delta^{min} \leq 2$); uniform grain distribution in the material body and on its surface; practically isotropic porosity of the abrasive material varying from 0.24 to 0.50 for different articles; cheapness of the abrasive material and its commercial availability in the form of about nine hundred types of hollow cylinders; and ability for being processed by industrial methods and tools.

Start-up–Adjustment Unit of the Combine "Orgneftekhimzavod." S. M. Kirov Chemical Technology Institute, Kazan. Translated from Teoreticheskie Osnovy Khimicheskoi Tekhnologii, Vol. 20, No. 6, pp. 805-812, November-December, 1986. Original article submitted April 9, 1985.

0040-5795/86/2006-0507$12.50

TABLE 1. Characteristics of the Structure of PRS made of Abrasive Materials

No. of specimen	Brand of specimen	Diameter of specimen, $D \cdot 10^3$, m	Mean logarithmic filtration surface, $S \cdot 10^3$, m^2	Coefficient of permeability, $K_{per} \cdot 10^{12}$, m^2	Porosity of specimen,* ε_{por}, %	Maximum pore size, $\delta^{max}_{por} \cdot 10^6$, m	Mean pore size, $\delta^{av}_{por} \cdot 10^6$, m	Coefficient of channel sinuosity, K_{sin}	Form factor of particles from (1), K_f	Mean weighted wall thickness of specimen, $\ell \cdot 10^3$, m
1	PVR-250	31.3	2.39	10.3	30(40.5)	227	33	6.8	1.94	10.4
2		33.6	2.5	11.8	32(36.0)	154	34	4.5	2.17	11.2
3		51.5	4.15	12.0	25(40.5)	218	33	8.7	1.36	16.4
4		51.5	4.15	25.0	32(40.5)	174	51	3.4	2.49	16.4
5		80.7	8.39	19.4	30(42.0)	178	45	3.9	2.56	8.2
6		81.0	8.48	21.1	34(42.0)	203	45	4.5	1.97	8.6
7	PVR-400	50.3	2.11	105.0	31(40.5)	683	104	6.6	1.88	15.0
8		63.0	3.82	33.7	40(42.0)	247	52	4.8	1.48	21.4
9		64.7	6.83	16.0	35(42.0)	247	38	6.5	1.58	19.8
10		65.0	6.76	16.5	40(42.0)	177	36	2.9	1.46	19.9
11		79.2	7.89	16.5	33(42.0)	324	36	9.0	1.54	24.5
12		81.9	5.16	30.0	33(37.5)	277	54	5.1	1.95	26.0

*Porosity values determined by the method of [5] are given within brackets.

Additional properties of abrasive materials [6] not reported in the literature were determined experimentally. Thus, the average pore diameter is $(40\text{-}55)\cdot10^{-6}$ m, its maximum being $(200\text{-}330)\cdot10^{-6}$ m. The coefficient of sinuosity of the channels depends on the wall thickness of the specimen and varies in the range 3.9 to 9.0. The form factor of the particles determined by the ratio obtained by simultaneously resolving Hagen–Poiseuille and Kozeny – von Karman equations

$$K_f = \frac{2.165(1-\varepsilon_{por})^{0.5}}{\varepsilon_{por}} K_{sin}, \quad (1)$$

averages 1.8 with not more than ±25% deviation of the individual values. The characteristics of the specimens used in the investigations are shown in Table 1. The values of ε_{por}, K_{per}, δ^{max}_{por}, and δ^{av}_{por} were determined by the methods prescribed in GOST 15079-69. The value of K_{sin} was determined by the method of [7, 8] and S was taken from [9].

The permeability of the PRS specimens made of abrasive materials was studied in the liquid flow range $2\cdot10^{-6}$ to $96\cdot10^{-6}$ m^3/sec, density 1010 to 1188 kg/m^3, and viscosity 1 to 26 Pa-sec; specimen rotation speeds 1 to 167 m/sec, and mean logarithmic filtration area $2.11\cdot10^{-3}$ to $8.48\cdot10^{-3}$ m^2.

Calculations using von Karman's equation [10] showed that, in the entire range of flow variations, physical properties of the medium, and the rpm of the specimens, the liquid flow through the porous wall of the specimen was laminary.

Test results showed (Fig. 1) that, at peripheral rotation speeds >3.5 m/sec, the permeability of the specimen depends on the liquid pressure in the chamber and on the material structure (regime I). Increasing the rotation speed reduces the influence of the material structure on the permeability of the PRS (regime II) and, at rotation speeds <10 m/sec, attains a self-modulating flow regime characterized by steady flow at a given pressure and viscosity of the liquid (regime III). The last regime is of utmost practical interest since intense drop formation on the sprayer surface is achieved in this regime. The liquid flow in the self-modulating flow regime could be calculated using empirical equations obtained by processing the experimental data [11]. At $\mu = 1\cdot10^{-3}$ to $6\cdot10^{-3}$ Pa-sec

$$Q = 33.7\cdot10^{-6}\Delta p(\mu\cdot10^3)^{-1.52}; \quad (2)$$

at $\mu = 6\cdot10^{-3}$ to $26\cdot10^{-3}$ Pa-sec

$$Q = 9.1\cdot10^{-6}\Delta p(\mu\cdot10^3)^{-0.30}. \quad (3)$$

The spraying of a hydrophilic liquid and the dispersion composition of the spray were studied photographically [12] using highly sensitive film (type 22) and developer D-19a. The results showed that, depending on the rotation speed of the PRS, a few characteristic regimes of liquid dispersion could be identified. Photographs of these regimes are given in [13, 14].

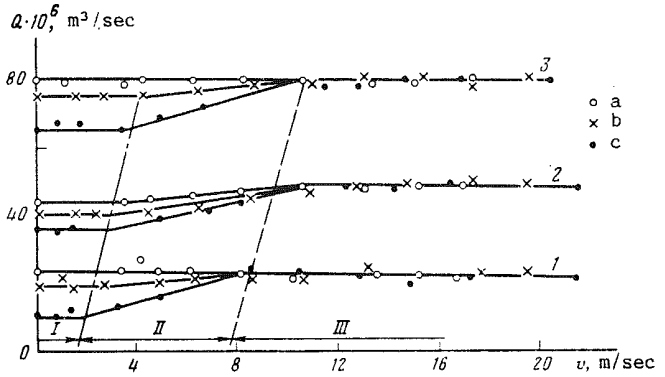

Fig. 1. Operational regimes of PRS made of abrasive material: 1) p = 14.7, 2) 39.2, and 3) 98.1 kPa; a) $K_k = 205 \cdot 10^9$ m³ (specimens 5 and 6, Table 1), b) $850 \cdot 10^9$ m³ (specimens 11 and 12), and c) $2895 \cdot 10^8$ m³ (specimens 1 and 4); and I-III) numbers of regimes.

At low rotation speeds of the PRS not exceeding 0.8 to 1.2 m/sec, a film is formed on the sprayer surface and flows downward; it accumulates on its lower edge in the form of a ridge. This ridge disintegrates into large globules and drops as noticed in a similar process on a disk [15]. Increasing the rotation speed of the PRS leads to a more uniform distribution of the liquid film along the height of the sprayer and formation of helical waves initially and later circular waves on its surface. These form the sources of jets disintegrating into drops. The dispersed liquid spray formed possesses a wide size range. On further increasing the rotation speed of the PRS, the film thickness and the sizes of the jet and of the drop formed from it decrease. Simultaneously, the extent of polydispersion decreases, d_{max}/d_{min} = 10-15 to 3-6. A laminary-jet regime of liquid spray is noticed in the range of rotation speeds 2 to 8 m/sec. Increasing the rotation speed beyond 8 m/sec leads to jet formation on a group of grains transforming into jet formation on individual grains. At speeds exceeding 12 m/sec, the jets disappear and the drop formation on the grains becomes stable. The extent of polydispersion is minimal, $d_{max}/d_{min} \leq 2$.

A comparison shows that the spraying pattern of hydrophilic liquids by the PRS is similar to that of liquid spray by the PRS made of cermets [1].

An analysis of the dispersion of the sprayed liquid in the drop formation regime on the grain showed (Fig. 2) that the drop size distribution is associated with the PRS grain distribution, $\delta_{max}/\delta_{min} \leq 2$.

In Table 2 are given the results of processing the experimental data obtained at different liquid loads and rotation speeds of the sprayers.

The average drop diameter in the regime of drop formation on the grain could be calculated from the equation derived by the method of analyzing the dimensions:

$$d_{32} = K[6\delta^{av}\sigma/(R\omega^2\rho)]^{1/4}. \quad (4)$$

Testing the adequacy of Eq. (4) using the experimental data showed that, at K = 0.52, it describes the experimental values with a deviation of not more than ±10% at 0.95 confidence level.

To calculate the average body-surface diameter of the drop (according to Sauter), the following equations were derived:

for PVR-250

$$d_{32} = (0.07 + 0.5(Q \cdot 10^3) + 0.57/v) \cdot 10^{-3} \text{ m}; \quad (5)$$

for PVR-400

$$d_{32} = (0.08 + 0.5(Q \cdot 10^3) + 1.37/v) \cdot 10^{-3} \text{ m}. \quad (6)$$

An analysis of the spray dispersion of aqueous solutions of surfactants, $\sigma = 29 \cdot 10^{-3}$ to $70 \cdot 10^{-3}$ N/m, showed (Fig. 3) that the extent of polydispersion is somewhat more compared with

TABLE 2. Results of Average Drop Size Measurements

$D \cdot 10^3$, m	$\delta \cdot 10^6$, m	$Q \cdot 10^6$, m^3/sec	v, m/sec	Average drop diameter d_{32}		Index of monodispersion, %
				experimental	from (4)	
Water ($\mu = 1{,}43 \cdot 10^{-3}$ Pa-sec, $\rho = 1010$ kg/m^3, $\sigma = 70 \cdot 10^{-3}$ N/m)						
PVR-250						
81.0	0.250	33.80	8.40	200	200	93
81,0	0,250	33,80	15.10	130	140	98
51,5	0,250	26,00	9.40	140	160	99
51,5	0,250	27,00	13.50	130	130	98
35,5	0,250	24.80	9,30	150	140	98
31.3	0,250	31.80	6.60	150	170	94
31,3	0,250	31,60	8.20	130	140	99
PVR-400						
79,2	0,400	33.80	14.50	180	160	96
64,7	0,400	27,10	13.50	200	170	95
81,9	0,400	28,20	17.20	160	150	97
Glycerin solution in water ($\mu = 25{,}56 \cdot 10^{-3}$ Pa-sec; $\rho = 1187$ kg/m^3; $\sigma = 60 \cdot 10^{-3}$ N/m)						
PVR-250						
81.0	0.250	30,0	8.40	190	180	80
81.0	0.250	30,0	12.60	160	170	92
81.0	0.250	30.0	15.60	130	120	98
51,5	0.250	30.0	8.40	160	160	94
51.5	0.250	30.0	9.40	150	150	95
51.5	0.250	30,0	10.80	140	130	97
PVR-400						
79.2	0.400	30.0	14.50	160	150	99
79.2	0.400	30.0	18.70	130	120	99
79.2	0.400	30.0	23.30	120	110	99
79.2	0.400	30.0	14.50	140	140	96
79.2	0.400	30.0	17.60	130	120	98
79.2	0,400	30,0	21.20	110	110	99

that of a pure water spray while the quality of spraying is independent of grain size of the specimens. For an average body-surface drop size of aqueous surfactant solutions

$$d_{32} = [(0.07 + 1.19\sigma) \cdot 10^3 + 0.88/v] \cdot 10^{-3} \text{ m}. \quad (7)$$

The results confirm that, under conditions of wetting, the grains of the abrasive material function as centers of drop formation. This is pointed out by the similarity of the integral curves of grain size distribution in the specimens and the drop sizes of the liquid sprayed and also by the relation of the average drop size with the average grain size of the specimen (Fig. 2). This mechanism of the spraying of hydrophilic liquids from the surface of a PRS made of abrasive material was implemented in the design of the monodispersed drop generator [16] in the form of two disks with metallic needles placed between them along the periphery. The needle tips are turned outward. The photographs of the liquid spray thus obtained confirmed that the drops formed at the needle tips, the drop size falling in a narrow range of 50 to 80 μm.

If in the drop formation regime at constant $R\omega^2$, the liquid flow through the PRS is steadily increased, the drop formation frequency on the grains of the sprayer begins to increase and the drops begin to fuse into a jet on attaining some critical flow Q_{cr}.

The liquid flow from a single center of drop formation (grain) corresponding to transition from the drop formation regime into a jet regime could be represented by the following equation as in [15]:

$$q = K_1 (\pi/2) \sqrt{R\omega^2 d^5}. \quad (8)$$

The number of drop formation centers

$$m = F(1 - \varepsilon_{por})/F_3. \quad (9)$$

Then the total fluid flow corresponding to the transition from drop forming to jet regime is

$$Q_{cr} = 0.24 K_1 F \omega (1 - \varepsilon_{por}) (d/\delta)^2 (Dd)^{0.5}. \quad (10)$$

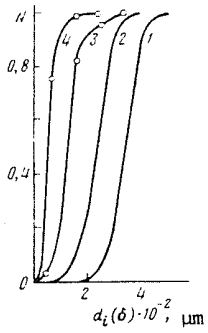

Fig. 2

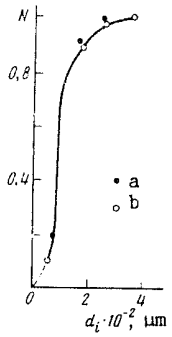

Fig. 3

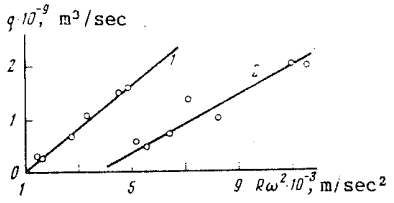

Fig. 4

Fig. 2. Integral curves of the distribution of drop sizes in the drop formation regime from a grain and of the material grains in the specimens [N, proportion of drop (grain)]: 1, 2) grain size distribution in PVR-400 and PVR-250 specimens [4]; 3) drop size distribution (PVR-400); $Q = 33.8\cdot10^{-6}$ m³/sec; $R\omega^2 = 5630$ m/sec², $D = 64.7\cdot10^{-3}$ m, and $d_{32} = 200$ μm; 4) drop size distribution (PVR-250); $Q = 27.1\cdot10^{-6}$ m³/sec, $R\omega^2 = 5630/\text{sec}^2$, $d_{32} = 130$ μm, and $D = 81.0\cdot10^{-3}$ m.

Fig. 3. Integral curves of drop size distribution of an aqueous surfactant solution ($\sigma = 45\cdot10^{-3}$ N/m, $Q = 30\cdot10^{-6}$ m³/sec, $R\omega^2 = 10{,}640$ m/sec², and $d_{32} = 165$ μm): a) PVR-250, $D = 80.7\cdot10^{-3}$ m; and b) PVR-400, $D = 64.7\cdot10^{-3}$ m.

Fig. 4. Value of critical flow: 1) PVR-250, and 2) PVR-400. Circlets denote the experimental data and continuous lines the values calculated using Eq. (10).

It was experimentally established that for PVR-250

$$K_1 = (0.11R\omega^2 - 137.8)\cdot10^{-3};$$

for PVR-400

$$K_1 = (0.052R\omega^2 - 206.5)\cdot10^{-3}.$$

In Fig. 4, the experimental values of Q_{cr} are compared with those calculated using Eq. (10).

When spraying aqueous solutions of surfactants, the wettability of the abrasive material is impaired thus changing the character of spraying of the liquid. Thus, in spite of a significant difference in the grain sizes of the sprayers PVR-250 and PVR-400, the disperse structure of the spray for both of them virtually coincides (Fig. 3). Considering this feature and also the fact that PVR-250 and PVR-400 possess practically identical average pore sizes (Table 1), it may be affirmed that the drop formation occurs from the pores when the wetting of the abrasive material by the liquid is weak. From this could be understood the experimentally noticed rise in the degree of polydispersion of the spray: It could be explained by the significant difference between the minimum and maximum pore sizes (Table 1).

Thus, a distinctive feature of the PRS made of abrasive material is that they effect the liquid spray on a solid surface but not in a gaseous phase which is characteristic of most industrial sprayers.

To optimize the PRS design, several problems including the shape and size of grains will have to be resolved. This could be done based on the equations for complete free surface energy of a 3-phase system in the absence of adsorption [17, 18]:

$$W = \sigma_{sg}F_{sg} + \sigma_{sl}F_{sl} + \sigma_{lg}F_{lg},$$

or taking into consideration the operational conditions of the PRS grains

$$W' = \sigma_{sl}f_{sl} + \sigma_{lg}f_{lg},$$

where f_{sl} and f_{lg} are the surfaces of the phase separation boundaries on the grain. Based on the surface tension determination at the phase separation boundary [19] and the minimum

W', it may be established that not only round particles, as established in [1, 3], but also acicular, rhomboid, rounded, and other particles oriented in the direction of liquid flow on the PRS surface should be used as elements of the working surface. The principle was used in the device of [16] in which the elements were acicular.

According to Eq. (4), at comparable conditions of $d \sim \delta(\delta_p)$, a surface consisting of uniform-sized elements is ideal from the view of monodispersion [16]. For industrial conditions, however, suffice to design a surface of elements of proximate sizes [20]; this agrees with the conclusions of [3].

Having examined quasistationary drop formation, it may be noticed that this process should proceed on a given element without interference from similar processes occurring on the adjoining elements. Evidently, this is possible only when the distance between two adjoining elements is not less than the diameter of the drop formed on that element under the given conditions. From Eq. (4), $R\omega^2$ is a decisive value in this process (from the design viewpoint). This conforms that the condition determining the size selection of the elements in [3] is only an exceptional case.

On the whole, the specifications for the PRS could be formulated as follows [7].

The effective (spraying) PRS surface should consist of different-sized elements projecting over it. Among these elements, the surface at the drop formation center (on wetting) should be minimal, i.e., tends to zero, and the elements should themselves alternate uniformly with the pores and their shape should promote flow only weakly when not wetted. The element (on wetting) should be oriented on the spraying surface toward the resultant forces which determine the liquid flow during drop formation. The distance between the drop forming elements on the PRS effective surface should be not less than the given drop diameter at the given centrifugal speed and the height of the element above the pore mouth (when not wetted) should be more than twice the given drop diameter.

On the whole, the PRS material should possess high porosity, strength, compatibility with other sprayer components, ease of repair, corrosion resistance, stability at high temperatures, and economy [17].

These specification were adopted when designing industrial spray-type equipment [20] which demonstrated high operational efficiency [21].

NOTATION

d, drop diameter, m; D and R, diameter and radius of the sprayer, m; F, sprayer surface, m^2; $K_k = 150(1 - \varepsilon_{por})^2 \ell/(S\varepsilon^2_{por}\delta^2_{por}K^2_f$, geometric characteristic of the porous body; p, liquid pressure, kPa; Δp, pressure drop in the sprayer, kPa; q, liquid flow rate from a single grain, m^3/sec; Q, volume flow rate of the liquid, m^3/sec; v, rotation speed of the sprayer, m/sec; δ and δ_{por}, sizes of grains and pores, m; μ, viscosity of the liquid, Pa-sec; ρ, density of the liquid, kg/m^3; σ, surface tension, N/m; and ω, peripheral speed of the sprayer, sec^{-1}.

LITERATURE CITED

1. P. Schmidt, Chem.-Ing. Tech., No. 5/6, 365 (1967).
2. H. Hege, Chem.-Ing. Tech., 36, No. 1, 52 (1964).
3. W. Gösselle, Chem.-Ing. Tech., No. 1/2, 37 (1968).
4. V. N. Bakul', Design Principles and Production Technology of Abrasive and Diamond Tools [in Russian], Mashinostroenie, Moscow (1975).
5. V. N. Lyubomudrov et al., Abrasive Tools and Their Production [in Russian], Mashgiz, Moscow–Leningrad (1953).
6. A. A. Kolesnik, F. A. Mustashkin, and N. A. Nikolaev, "Dispersing capacity of porous rotary sprayers made of abrasive material," Paper filed at BU VINITI, No. 10, 118 (1983).
7. S. M. Solonin et al., "Determining the pore sizes of filter materials made up of nonspherical powders," Poroshk. Metall., No. 1, 38 (1971).
8. S. M. Solonin et al., "Porous metals from electrolytic chromium," Poroshk. Metall., No. 7, 34 (1971).
9. A. S. Berkman et al., Porous Penetrable Ceramics [in Russian], Gosstroiizdat, Leningrad (1966).
10. P. G. Romankov and M. I. Kurochkina, Hydromechanical Processes in Chemical Engineering [in Russian], Khimiya, Leningrad (1982).

11. A. A. Kolesnik, F. A. Mustashkin, E. A. Komarov, and N. A. Nikolaev, "Determining the flow characteristics of porous rotary liquid sprayers," in: Hydromechanics and Heat Transfer in Heating and Ventilation Equipment [in Russian], Kazan' (1981), p. 58.
12. F. A. Mustashkin, N. A. Nikolaev, and A. M. Nikolaev, "A study of liquid dispersion in eddy-type columns," Izv. Vyssh. Uchebn. Zaved., Khim. Tekhnol., No. 9, 1370 (1970).
13. A. A. Kolesnik, F. A. Mustashkin, and N. A. Nikolaev, "Mechanism of liquid spraying by porous rotary sprayers made of abrasive materials," Paper filed at BU VINITI, No. 10, 118 (1983).
14. D. G. Pazhi and V. S. Galustov, Principles of Liquid Spraying [in Russian], Khimiya, Moscow (1984), p. 155.
15. V. F. Dunskii and N. V. Nikitin, "Mechanical spraying of liquids," in: Aerosols in Plant Protection [in Russian], Kolos, Moscow (1982), p. 122.
16. A. A. Kolesnik, F. A. Mustashkin, et al., "Drop generator," USSR Inventor's Certificate No. 1052271, Byull. Izobr., No. 41 (1983).
17. A. A. Kolesnik, F. A. Mustashkin, and N. A. Nikolaev, "Principles of designing porous rotary liquid sprayers," in: IIIrd All-Union Conference "Modern Machinery and Equipment for Chemical Industry," Chimkent (1983), p. 54.
18. B. D. Summ and Yu. V. Goryunov, Physical and Chemical Principles of Wetting and Flow [in Russian], Khimiya, Moscow (1976).
19. A. D. Zimon, Adhesion of Liquids and Wetting [in Russian], Khimiya, Moscow (1974).
20. A. A. Kolesnik, N. A. Nikolaev, et al., "Porous rotary sprayer," USSR Inventor's Certificate No. 738679, Byull. Izobr., No. 21 (1980).
21. A. A. Kolesnik, F. A. Mustashkin, et al., "Industrial testing of equipment with porous rotary liquid sprayer," Prom. Sanitarnaya Ochistka Gazov, No. 6, 1 (1982).

OPTIMIZATION OF CHEMICAL ENGINEERING SYSTEMS WITH INDETERMINATE INFORMATION

V. V. Kafarov, V. V. Zolotorev, V. N. Bogdanov, A. M. Chekalin, and V. V. Garnov

UDC 65.018.2.002.2

The concept of three types of information uncertainty in chemical engineering systems (CES) optimization problems is introduced. The basic disadvantages of traditional optimization methods and existing approaches to the solution of optimization problems are formulated with a consideration of information uncertainty factors. A method of calculating the mean-integral optimization criterion is proposed and used to develop a CES optimization algorithm that permits the determination of optimum values for the parameters of objects studied under real operating conditions. The effectiveness of the algorithm is demonstrated by solving test problems.

Traditional methods of solving optimization problems often provide unsatisfactory results from the practical point of view. This condition can stem from neglecting a series of objectively present uncertainty factors when the original problem is formulated. The major uncertainty factors are: 1) uncertainty in the optimization parameters because it it impossible to stabilize them precisely at an optimum level, which makes it necessary to determine an optimum position within a permissible search region (PSR) that is no longer a point (which limits traditional methods) and in some region of uncertainty whose dimensions depend on how much the optimization parameters can deviate from their own nominal values; 2) uncertainty in the parameters of the optimization criterion due to the fact that several quantities necessary for their calculation (such as the parameters of mathematical models) can be assigned with only a certain degree of accuracy, making it necessary to account for possible deformations in the hypersurface of a criterion due to fluctuations in the quantities that make it up; 3) uncertainty in the limitation parameters, often because it is impossible to assign

D. I. Mendeleev Moscow Chemical Technology Institute. Translated from Teoreticheskie Osnovy Khimicheskoi Tekhnologii, Vol. 20, No. 6, pp. 813-824, November-December, 1986. Original article submitted April 2, 1986.

